ANALYSIS OF ELASTOPLASTIC FLOWS ON IRREGULAR TRIANGULAR GRIDS WITH RESTRUCTURING

V. N. Aptukov and A. V. Fonarev

UDC 539.3

1. Introduction. Problems in dynamic deformation of solids can be solved by various methods. This variety reflects the wide range of high-velocity deformation processes and diverse engineering applications. There are no universal techniques. Each method is limited to a narrow range of effective applications. A general review of the state of the art in numeric modeling of nonstationary elastoplastic dynamic problems can be found in [1].

These methods can be classified according to several characteristics, depending on the type of processes analyzed. Explicit methods are employed in studies of wave processes. Implicit methods are used to solve nonwave dynamic problems with small gradients. There are walkthrough calculation schemes with artificial or approximation viscosity, and plans explicitly isolating discontinuity surface (characteristic methods). Modeling of processes with a wide variation in the form of the region analyzed has remained an unmet challenge. With an Eulerian grid, difficulties are encountered in satisfying the boundary conditions on contact surfaces. Large form variations also make it difficult to utilize purely Lagrangian grids. In response to this need, all kinds of "hybrid" schemes have been suggested [2, 3].

A simple and effective method for analysis of elastoplastic flows is the Wilkins scheme [4]. Applications of this method to problems with large form variations require restructuring the grid in the region of strong distortions. A special case of restructuring with elimination of the distorted elements on a quadrangular grid has been realized in [5]. Subsequently, the authors of [5] resorted to grid restructuring for explicit isolation of the surface of a separation crack [6]. An alternative algorithm, which takes into account fissuring or sliding surfaces by splitting the nodes of a grid, was developed in [7, 8]. An algorithm of irregular restructuring of the grid developed for the finite-element method in [9] is more effective. The topology of regular grids becomes unsuitable with large distortions and for approximations of geometrically complex regions.

In this connection, it is desirable to construct and implement a Wilkins procedure on irregular triangular grids with a general restructuring algorithm. A first attempt at implementing such an algorithm was undertaken in [10].

2. Triangulation. The method of natural approximation of derivatives [4] imposes no constraints on the type of difference grid. For regions of a complex geometry or with large distortions in the calculation grid it is convenient to take an irregular triangular grid for the starting point. In fact, the regularity requirement is in conflict with the desire to improve approximation accuracy in the local regions where restructuring is undertaken.

Several algorithms of automatic triangulation for complex regions have been proposed in [11, 12]. Their applications are determined by the type of problem, the type of region, etc. The following sequence of steps in triangulation seems appropriate: dividing the initial region into subregions in accordance with the physical essence of the problem or its geometry, constructing in each subregion a coarse grid independent of the other subregions, condensing the grid by introducing new nodes and/or modifying the topology, smoothing the grid for the entire region or separately by subregions.

This sequence of steps has been implemented as modules programmed in Fortran. The quality of the grid depends mainly on the first two steps. The basic module of the second step involves triangulation by reduction of the region [3] and irregular restructuring in grid formation.

The operation of grid smoothing is accomplished by successive transfer of each internal node of the grid to the center of gravity of its "star." The transfer magnitude depends

---

Perm. Translated from Zhurnal Prikladnoi Mekhaniki i Tekhnicheskoi Fiziki, No. 6, pp. 109-115, November-December, 1990. Original article submitted May 16, 1989.

0021-8944/90/3106-0901$12.50

on the iteration number and the weight of the node which are specified in advance as grid constants.

3. Irregular Restructuring and Interpolation. A program for irregular restructuring has been created to improve the grid in the local region of large form variations or for initial adaptation of the grid to specifics of solution. Restructuring algorithms have been discussed in several publications (in particular, [6, 9, 11, 14, 15]). Typically, grid improvement is achieved by diminution or aggregation of the mesh.

In the present paper, we operate with an expanded set of basic restructuring operations [9, 11]: change of the diagonal; introduction of a new node on an edge; elimination of an edge; a new triangulation of a "star" of elements; and introduction of a new inner node. The capacities of the algorithm are expanded by taking into account a larger number of nodes and elements that contribute to local grid enhancement. The function of the measure of element distortion proposed in [9] is used as the grid distortion criterion that determines the need for restructuring.

In interpolation of variables from the old grid to the new one, a conservative interpolation algorithm makes use of the mass conservation integral [16]

$$m_k = \int_{V_k} \rho(\mathbf{r})\,dV \tag{1}$$

[m_k and V_k are the mass and volume of the new element; $\rho(\mathbf{r})$ is the density distribution function for the state of the old grid].

On the basis of (1), we calculate the volume increment ΔV_{ij} in the new element i relative to the old element j. Interpolation of variables (except for mass, density, and volume) with the aid of ΔV_{ij} appears as

$$\overline{\psi}_i = \frac{1}{\overline{V}_i} \sum_{j=1}^{n} \Delta V_{ij} \psi_j, \quad i = \overline{1, m},$$

where $\overline{\psi}_i$, ψ_j are the values of the variable on the new and old grids, respectively; n and m are the number of elements in the new and old grids in the fragment being restructured.

Calculation of volume increments ΔV_{ij} encounters difficulties with finding, on uncoordinated grids, a portion of the volume of the old element j incorporated in the new element i. To this end, a net of points (approximately 100 points per element) is "injected" into the old grid. Each point has a volume of its own. Its value depends on the number of points falling upon the old element. The volume increment ΔV_{ij} is the sum of volumes of the points that are shared by the new element i and the old element j.

The numbers of nodes and elements can change as a result of restructuring. Velocities are interpolated linearly by the velocities of three old nodes surrounding a given new node.

4. Differential Equations and Their Approximations. Difference approximation has been employed to find node velocities on an irregular triangular grid [17]. Deformation rates have been determined with the use of an integral representation of partial derivatives [4] taking into account a triangular grid [17]. Other difference relations and time integrations have been constructed similarly in [4].

The topology of the grid is described by indirect addresses which link each element number with the numbers of three surrounding nodes. The description of connections is implemented in the form of a list. Examples of list applications can be found in [11, 13]. With indirect addressing, the following operations are simplified: use of arbitrary triangular grids; introduction and elimination of nodes and elements; irregular restructuring; and adjustment for cracks.

5. Test Calculations. For verification of the general algorithm, we will examine the collision of deformable rods with a rigid wall.

In the first example, we will consider in a plane two-dimensional statement, the impact at 45° and the flow spread of an aluminum striker rectangular in plan with zero yield strength. The impact velocity is v_0 = 1 km/sec; the initial density is ρ_0 = 2.7 g/cm^3; the

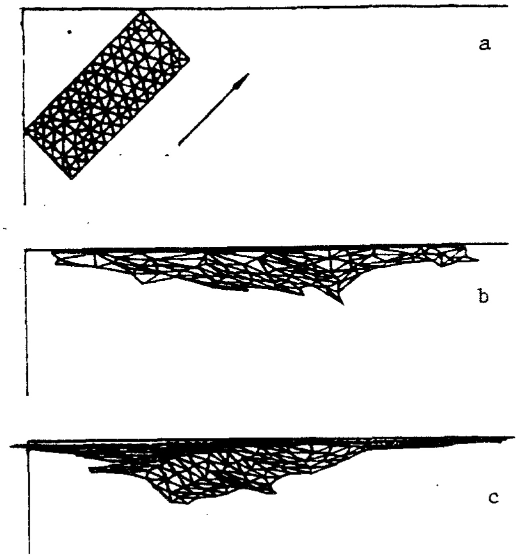

Fig. 1

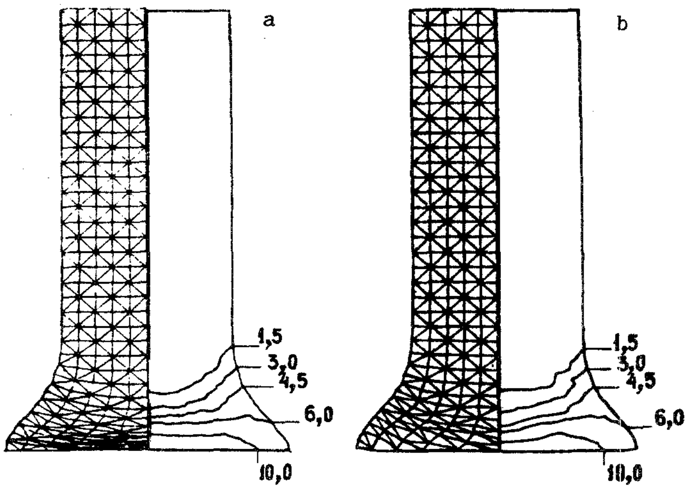

Fig. 2

parameters of the characteristic equation $p = A(\rho_0/\rho)^n - B$ are the following: $n = 3.8$, $A = B = 23.7$ GPa; bulk modulus $K = 74.4$ GPa; shear modulus $G = 28.5$ GPa.

Figure 1 shows the initial position of the striker (a) and its position at dimensionless time $t = 4$ sec with restructuring (b) and without it (c). For calculations until the time $t = 4.2$ sec without restructuring, 1840 steps were required; 1000 steps were required to bring the process up to $t = 5.7$ sec. While the time step reduction with restructuring was $\Delta t/\Delta t_0 = 0.4$, without restructuring it was $\Delta t/\Delta t_0 = 0.09$. Thus, further calculation without restructuring is practically impossible. A comparison of the pulse components P_x/P_0 and P_y/P_0 in calculations with and without restructuring for times $t = 1, 2, 3$, and 4 sec ascertained a practically perfect match. The total energy errors $1 - E/E_0$ for the same times were 0.02, 0.07, 0.065, 0.09 and 0.025, 0.045, 0.06, and 0.07, respectively. For the time $t = 5.7$ sec, a total of 14 restructurings were executed.

In the second example, we considered in an axisymmetric statement the impact of a cylindrical aluminum rod against a rigid wall. The yield strength of aluminum $Y_0 = 0.5$ GPa. Figure 2 illustrates deformable rods and the lines of equal deformation intensity levels (%) without (a) and with (b) restructuring of the grid at final time points. The restructuring obviously preserves the qualitative and quantitative characteristics of the process.

In series of calculations modeling an impact of deformable rods against a rigid wall [18], the deviation of rod shortening for $v_0 \sim 400$ m/sec did not exceed 3% and for $v_0 \sim 600$ m/sec did not exceed 10%.

6. Interaction of a Striker with Deformable Plate. A rigid cylindrical striker penetrates a plate of aluminum alloy 1911, hitting the plate with its flat endface. The mechanical characteristics of the alloy were given in [19]. The ratios of striker diameter to plate thickness and to plate diameter are 0.3 and 0.1, respectively. In the calculations we took account of the thermal effects due to volume change ΔV and plastic work of the forming process:

$$\rho c\Delta T = -3\alpha KT\Delta V + (1/\sqrt{3})\sigma_u\Delta\varepsilon_u, \tag{2}$$

where c is the specific heat capacity; ΔT is the temperature increment; α is the thermal expansion coefficient; σ_u and ε_u are the stress and strain rates; K is the current dilation modulus.

In relation (2),

$$\alpha(T) = \alpha_0(1 + 0.2T/T_{p\ell}),\ c(T) = c_0(1 + 0.3T/T_{p\ell}) \tag{3}$$

[$\alpha_0 = 2.2\cdot10^{-5}$ deg^{-1}, $c_0 = 5.75$ kJ/(kg·deg), $T_{p\ell} = 600$°C].

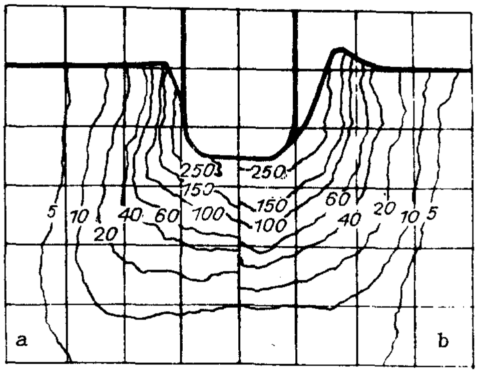

Fig. 3

The yield strength of the plate material is assumed to be a function of the temperature, the accumulated strain, and the strain rate:

$$\sigma_u = \exp[-1{,}4(2{,}07T/T_{p\ell})^{1/8}][\sigma_s(\varepsilon_u) + \sigma_\mu(\dot{\varepsilon}_u)]; \quad (4)$$

$$\sigma_s(\varepsilon_u) = \sigma_s^0[k - (k-1)\exp(b\varepsilon_u)]; \quad (5)$$

$$\sigma_\mu(\dot{\varepsilon}_u) = \begin{cases} \mu_T\dot{\varepsilon}_u, & \dot{\varepsilon}_u \leqslant J, \\ \mu_T J + \mu_T \dfrac{J}{1-B}\left[\left(\dfrac{\dot{\varepsilon}_u}{J}\right)^{1-B} - 1\right], & \dot{\varepsilon}_u > J, \end{cases} \quad (6)$$

where $\sigma_s{}^0$ = 0.45 GPa; b = −25; k = 1.1-1.5; J = 100 sec^{-1}; B = 0.65-0.7; $\mu_T = \mu_0(1-0.32\ T/T_{p\ell})$; $\mu_0 = 0.25\cdot10^{-3}$ GPa·sec.

The temperature behavior in (3) and (4) is formulated on the basis of reference data from [20]. Relation (5) approximates experiments with alloy 1911. Expression (6), which takes into account the effect of the rate of deformation, is borrowed from [21].

The temperature effect on the shear modulus is expressed by

$$G = G_0\exp[-1.4(1.5T/T_{p\ell})^3].$$

The computer experiment indicated that the inclusion of temperature in the defining equations for the aluminum alloy at mean impact velocities of v_0 ~ 300-800 m/sec had little effect on the penetration process. It resulted in a stronger localization of deformations near the side surface and the crater bottom. The temperature distribution near the crater was similar to that of the deformation rates ε_u. Thus, when the striker penetrates deep into the plate at medium velocities the energy dissipation asociated with plastic strains is the principle contributor to the temperature-related change.

A study of the effect of deformational strengthening and the yield strength upon the penetration process indicated the following. At small k ~ 1.05 (for slightly reinforcible material) the growth of $\sigma_s{}^0$ (with analysis of the variants of $\sigma_s{}^0$ = 0.4; 0.5; 0.6 GPa) has virtually no effect on the strain distribution around the crater, although the resistance to penetration is slightly increased. At k = 1.4 (for a strongly reinforcible material) the region of pronounced radial deformations is expanded. For example, the boundary of

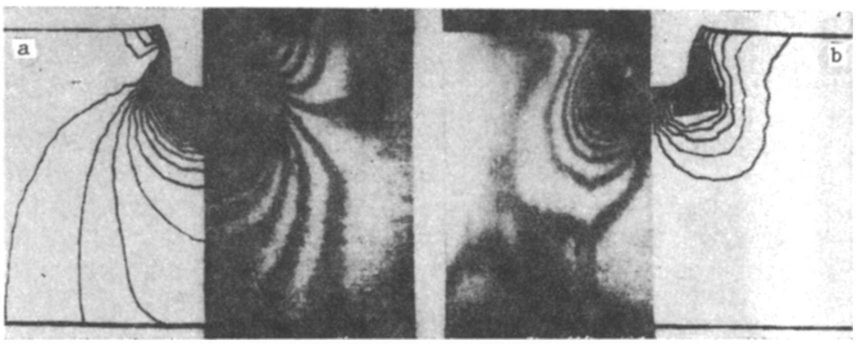

Fig. 4

deformation intensity region ε_u = 10% relative to the radius (relative to the striker diameter) is 1.6 for the material without reinforcement and 2.4 for the material with reinforcement. In both cases, the deformed zones under the striker endface are equal. A large volume of the plate is involved in the work for the intensely reinforcible material due to its nonuniform resistance to plastic deformation.

We investigated the effect of the velocity of the striker passage through a certain plate cross section upon the distribution of strains near the crater. The data indicate slight differences entirely due to the behavior of the rear facing layers. Thus at a current crater depth equal to half the plate thickness for v_0 = 550 and 800 m/sec the reverse bulge on the plate is smaller in the latter case, while the inertial outflow and the expansion of the crater near the face surface is, of course, smaller in the former case. With increasing impact velocity the conical region of maximum displacement under the striker is slightly narrowed. This is illustrated by the isotherms and the crater cross section for v_0 = 300 m/sec (a) and 800 m/sec (b) at a penetration depth on the order of 1.5 striker radii (Fig. 3).

To estimate the effect of penetration velocity on the deformation pattern and test the calculation algorithm, we compared the processes of static penetration (experimental) and dynamic penetration (calculated) with v_0 = 300 m/sec. Figure 4 shows the calculated and experimental lines of equal displacements U_z (a) and U_r (b). (The experimental data were kindly provided by Yu. Yu. Lesnichenko). The experimental method with moiré bands is similar to the technique described in [19, 22]. A look at Fig. 4 validates this computer program. The figure also shows the similarity of deformation processes during static and dynamic penetration of a striker into a plastic metal sheet at low and medium velocity of impact.

LITERATURE CITED

1. V. N. Kukudzhanov, "Numeric modeling of dynamic deformation and destruction processes," Usp. Mekh., 8, No. 4 (1985).
2. I. B. Petrov, Numeric Analysis of Penetration Processes with Mobile Calculation Grids [in Russian], Dep. VINITI, No. 103-82, January 8, 1982, Moscow (1982).
3. K. I. Zapparov and V. N. Kukudzhanov, "Mathematical modeling of impulse deformation interaction and destruction of elastoplastic bodies [in Russian]," Preprint, No. 280, Institute of Problems in Mechanics, USSR Academy of Sciences, Moscow (1986).
4. M. L. Wilkins, "Calculations of elastoplastic flows," in: Computational Methods in Hydrodynamics [Russian translation], Mir, Moscow (1967).
5. A. I. Gulidov and V. M. Fomin, "A modification of the Wilkins Method for solution of collision problems [in Russian]," Preprint, No. 49, Institute of Theoretical and Practical Mechanics, USSR Academy of Sciences, Siberian Branch, Novosibirsk (1980).
6. A. I. Gulikov, V. M. Fomin, and I. P. Shabalin, "Algorithm for restructuring of the difference grid in numeric solution of collision problem with crack formation," in: Proceedings of a Conference on Numeric Methods of Solution of Elasticity and Plasticity Problems [in Russian], Inst. Teor. Prikl. Mekh., Sib. Otd. Akad. Nauk SSSR, Novosibirsk (1982).
7. B. E. Ringers, "New sliding surface techniques enable Lagrangian code to handle deep target penetration/perforation problems," Lect. Notes Eng., 3 (1983).
8. V. A. Gridneva and M. M. Nemirovich-Danchenko, "A method of splitting of grid points for numeric calculation of the fracturing of solids [in Russian]," Dep. VINITI, No. 3258-83, Tomsk (1983).
9. A. I. Sadyrin, "Algorithm of irregular restructuring of plane triangular grids in the finite-element method," in: An Interuniversity Compendium on Applied Problems of Strength and Plasticity [in Russian], Gorky State University, Gorky (1985).
10. A. V. Fonarev, "Irregular triangular difference grids used in the solution of problems of impulse deformation of elastoplastic bodies," in: Proceedings of the 6th National Conference on the Theoretical Principles and Construction of Numeric Algorithms for Solution of Problems in Mathematical Physics [in Russian], Izd-vo GGU, Gorky (1986).
11. V. I. Polezhaev and A. I. Fedoseev, "Finite-element method in hydromechanical and heat, and mass exchange problems [in Russian], Preprint, No. 160, Institute of Problems in Mechanics, USSR Academy of Sciences, Moscow (1980).

12. W. C. Thasker, "A brief review of techniques for generating irregular computational grids," Int. J. Numer. Meth. Eng., No. 16 (1980).
13. S. É. Umanskii, "An algorithm and a program for triangulation of a two-dimensional region of an arbitrary shape," Probl. Prochn., No. 6 (1978).
14. M. C. Rivera, "Algorithm for refining triangular grids suitable for adaptive and multi-grid techniques," Intern. J. Numer. Meth. Eng., 20, No. 4 (1984).
15. W. H. Frey, "Selective refinement: A new strategy for automatic node placement in graded triangular meshes," Int. J. Numer. Meth. Eng., 24, No. 3 (1987).
16. J. K. Dikowicz, "Conservative rezoning (remapping) for general quadrilateral meshes," J. Comp. Phys., 54, No. 3 (1984).
17. A. V. Fonarev, "Arbitrary triangular difference grids used to solve problems of pulse deformation of elastoplastic bodies," in: Models of Deformation and Destruction of Composite Materials [in Russian], UrO Akad. Nauk SSSR, Sverdlovsk (1988).
18. M. L. Wilkins and M. W. Guinan, "Cylinder impact on a rigid target," in: Mechanics: A Collection of Translations [Russian translation], Mir, Moscow (1973).
19. V. N. Aptukov, V. F. Kashirin, R. T. Murzakaev, et al., "Moiré method used in studies of separation fracturing," Dokl. Akad. Nauk SSSR, 290, No. 2 (1986).
20. C. W. Besserer, Missle Engineering Handbook, Van Nostrand Reinhold, New York (1958).
21. V. N. Aptukov and P. K. Nikolaev, "Wave propagation in thermoelastic viscoplastic materials," in: The Dynamics of a Continuous Medium: A Collection of Papers. 1 [in Russian], Akad. Nauk SSSR, Sib. Otd. Inst. Gidrodin. (1984).
22. V. N. Aptukov and Yu. Yu. Lesnichenko, "Experimental studies of aluminum alloy plate resistance to static penetration of a rigid indenter," in: Dynamics and Strength of Mechanical Systems: An Interuniversity Compendium [in Russian], Perm Polytechnical Institute, Perm (1984).

AXIAL COMPRESSION OF AN INHOMOGENEOUS CONE

M. A. Zadoyan and N. B. Safaryan UDC 539.376

A concentrated axial force is applied to the apex of an infinite cone. The material is assumed to be incompressible, inhomogeneous, and conforming to the power law of reinforcement. The compression of this cone is investigated. The corresponding homogeneous problem was studied in [1, 2].

Differential equations of equilibrium for an axisymmetric deformation in spherical coordinates in the usual notations appear as

$$\frac{\partial\sigma_r}{\partial r}+\frac{1}{r}\frac{\partial\tau_{r\theta}}{\partial\theta}+\frac{1}{r}(2\sigma_r-\sigma_\theta-\sigma_\varphi+\tau_{r\theta}\operatorname{ctg}\theta)=0,$$
$$\frac{\partial\tau_{r\theta}}{\partial r}+\frac{1}{r}\frac{\partial\sigma_\theta}{\partial\theta}+\frac{1}{r}[(\sigma_\theta-\sigma_\varphi)\operatorname{ctg}\theta+3\tau_{r\theta}]=0,\tag{1}$$
$$\frac{\partial\tau_{r\varphi}}{\partial r}+\frac{1}{r}\frac{\partial\tau_{\theta\varphi}}{\partial\theta}+\frac{1}{r}(3\tau_{r\varphi}+2\tau_{\theta\varphi}\operatorname{ctg}\theta)=0.$$

The reinforcement law for this material is

$$\sigma_0=k\omega(\theta)\,\varepsilon_0^m,\quad 0<m<1,\tag{2}$$

where k is a constant; $\omega(\theta)$ is a given function determined experimentally;

$$\sigma_0=\frac{1}{\sqrt{6}}\sqrt{(\sigma_r-\sigma_\theta)^2+(\sigma_\theta-\sigma_\varphi)^2+(\sigma_\varphi-\sigma_r)^2+6\left(\tau_{r\theta}^2+\tau_{\theta\varphi}^2+\tau_{r\varphi}^2\right)},$$
$$\varepsilon_0=\sqrt{\frac{2}{3}}\sqrt{(\varepsilon_r-\varepsilon_\theta)^2+(\varepsilon_\theta-\varepsilon_\varphi)^2+(\varepsilon_\varphi-\varepsilon_r)^2+6\left(\gamma_{r\theta}^2+\gamma_{\theta\varphi}^2+\gamma_{r\varphi}^2\right)}$$

Erevan. Translated from Zhurnal Prikladnoi Mekhaniki i Tekhnicheskoi Fiziki, No. 6, pp. 115-118, November-December, 1990. Original article submitted November 9, 1988; revision submitted May 4, 1989.

